BIOCHEMISTRY
including biophysical chemistry & molecular biology

ARTICLE

pubs.acs.org/biochemistry

A Circumventing Role for the Non-Native Intermediate in the Folding of β-Lactoglobulin

Kazumasa Sakurai,[†] Shunsuke Fujioka,[†] Tsuyoshi Konuma,[†,§] Masanori Yagi,[‡] and Yuji Goto*[,†]

[†]Institute for Protein Research, Osaka University, 3-2 Yamadaoka, Suita, Osaka 565-0871, Japan

[‡]Research Institute for Microbial Diseases, Osaka University, 3-1 Yamadaoka, Suita, Osaka 565-0871, Japan

Supporting Information

ABSTRACT: Folding experiments have suggested that some proteins have kinetic intermediates with a non-native structure. A simple Gō model does not explain such non-native intermediates. Therefore, the folding energy landscape of proteins with non-native intermediates should have characteristic properties. To identify such properties, we investigated the folding of bovine β-lactoglobulin (βLG). This protein has an intermediate with a non-native α-helical structure, although its native form is predominantly composed of β-structure. In this study, we prepared mutants whose α-helical and β-sheet propensities are modified and observed their folding using a stopped-flow circular dichroism apparatus. One interesting finding was that E44L, whose β-sheet propensity was increased, showed a folding intermediate with an amount of β-structure similar to that of the wild type, though its folding took longer. Thus, the intermediate seems to be a trapped intermediate. The high α-helical propensity of the wild-type sequence likely causes the folding pathway to circumvent such time-consuming intermediates. We propose that the role of the non-native intermediate is to control the pathway at the beginning of the folding reaction.

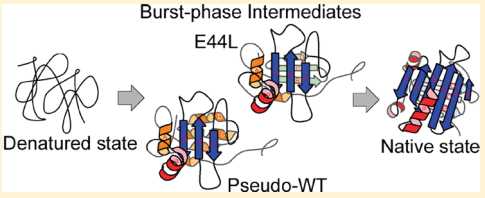

Experiments have shown that, although small proteins show two-state folding, the folding of proteins with more than ~100 residues involves a number of intermediate species.[1−5] The two-state folding process for small proteins is seemingly consistent with a simple Gō model, which is ideal for predicting an energy landscape with a completely smooth surface. On the other hand, larger proteins tend to have greater frustration in their native conformation. Such frustrations likely lead to a more rugged energy landscape for protein folding, which results in the involvement of folding intermediates.[6,7] It is not clear whether such frustrations within the native conformation were introduced by incidental mutations or by evolutional pressure.

Some researchers refer to an intermediate state to explain positive effects. Several folding schemes with specific intermediates, including the hydrophobic collapse model[8,9] and the framework model,[3,10] have been suggested. The intermediates observed in these models occur in the early stage of the folding process and are assumed to reduce the conformational space to be searched for the final, native state. On the other hand, intermediates with non-native interactions have been shown to stabilize unfolded forms in the absence of a denaturant, demonstrating that much of the conformational search for the native structure occurs during the very initial events of folding.[11,12] The formation of non-native contacts might increase the rate of folding by minimizing the search for the native state to fewer dimensions.[13]

In addition, some research groups suggested that the temporary formation of an α-helical intermediate is a general property of the β-sheet proteins.[14,15] Chikenji et al.[15] presented this idea based on a simulation of the lattice model of a β-barrel protein with a Gō potential. Chen et al.[14] also suggested the idea from an analysis of the amino acid sequence of β-sheet proteins based on Lim's theory.[16] This theory suggests that the sequences of β-sheet proteins inherently have the potential to form an amphiphilic extended helix of ~3.0 residues/turn as well as amphiphilic α-helix of 3.6 residues/turn in the early stages of folding and that the potential to form the extended helix should be higher than that to form the α-helix for rapid folding because the extended helix is the intermediate in the folding process leading to the final β-sheet structure.

We have been investigating the folding of bovine β-lactoglobulin (βLG) to address the significance of a non-native folding intermediate. βLG is a major whey protein abundant in bovine milk.[17,18] It consists of 162 amino acid residues (18 kDa) and contains two disulfide bonds (residue 66−residue 160 and residue 106−residue 119) and a free thiol (residue 121). βLG is a predominantly β-sheet protein consisting of nine β-strands (A−I), of which strands A−H form an up-and-down β-barrel, and one major α-helix at the C-terminal end.[19−21] Among its properties, including the binding of small hydrophobic compounds[22] and formation of a noncovalent homodimer,[23] is a transient accumulation of intermediates with non-native α-helices, followed by conversion to the native β-sheet structure, during the refolding process.[24−26]

Previous studies have clarified the mechanism responsible for the formation of the non-native α-helical intermediate as follows.

Received: February 16, 2011
Revised: May 26, 2011
Published: June 16, 2011

Non-native α-helices form at the N-terminal half of βLG from strands A to D in the early stages of refolding via a local α-helical preference.[24,27−29] Concomitantly, key elements of the native structure are also formed at strands F−H and the major helix.[26] It was reported that this intermediate assumes a compact conformation,[30] which might result from the formation of the native and non-native secondary structures. After this stage, the local interactions are substituted with more stable, nonlocal interactions forming the native β-structure.

To investigate the role of the non-native intermediate in βLG's folding, we prepared βLG mutants whose secondary structure propensity is modified, believing that the α-helical propensity of the sequence is coupled with the stability of the non-native intermediate. Then, we measured the folding kinetics of the mutants by stopped-flow CD as well as the stability of the intermediates in Gdn-HCl titration experiments. The folding pathway changed with the α-helical propensity. It is noted that Lim's theory, which was introduced above, was found to explain the importance of the non-native intermediate and the changes in the folding behaviors caused by the mutations observed in this paper. We suggest that the βLG molecule circumvents a kinetically trapped state through the non-native α-helical conformation, making its folding more rapid. Our results will provide further insights into the role of folding intermediates.

MATERIALS AND METHODS

Construction of an Expression Plasmid for C121A βLG. An *Escherichia coli* expression system was selected for producing C121A βLG and its mutants. cDNA encoding C121A βLG within plasmid pPIC/βLG C121A, which was constructed for the *Pichia pastoris* expression system,[31] was amplified by PCR using *Pfu* Turbo DNA polymerase (Stratagene Cloning Systems, La Jolla, CA). The amplified DNA fragment was cloned into *E. coli* expression vector pAED4[32] using *Eco*RI and *Nde*I. A Met residue was always present at the N-terminal position of the recombinant protein; that is, the amino acid sequence of the N-terminus is Met0-Ala1-Tyr2-Val3-Thr4-Gln5-... Other mutations, G17E and E44L, were introduced using the QuikChange site-directed mutagenesis kit (Stratagene) as described previously.[33]

Expression and Purification of C121A βLG and Its Mutants. The mutants were expressed in *E. coli* BL21(DE3) pLysS (Novagen, Inc., Madison, WI). C121A βLG and the other mutants accumulated in inclusion bodies. As these βLG molecules can contain non-native disulfide bonds, disulfide bonds were reduced by dissolving the inclusion bodies in a 9 M urea solution containing 20 mM DTT. Then, this solution was diluted 50-fold in 30 mM Tris-HCl (pH 8.0) containing 2 mM cysteine, 2 mM cystine, and 1 mM EDTA and stirred for 1 day at 4 °C for the formation of correct disulfide bonds and refolding of proteins. The refolded sample was applied to a column of CM Sepharose CL-6B (GE Healthcare UK Ltd., Buckinghamshire, England) equilibrated with 50 mM glycine-HCl (pH 3.0), and the proteins were eluted with a linear gradient of NaCl (0 to 1 M). The fraction containing the major peak was applied to a Resource S column (GE Healthcare) equilibrated with 50 mM glycine-HCl (pH 3.0), and the proteins were eluted with a linear gradient of NaCl (250 to 750 mM). The fraction containing the major peak was dialyzed against 4 mM HCl and lyophilized. Monomeric concentrations of C121A βLG and its mutants were determined by measuring UV absorption using a U-3000 spectrophotometer (Hitachi, Tokyo, Japan). The protein extinction coefficient ($\varepsilon = 18260\ M^{-1}\ cm^{-1}$) was calculated from the amino acid sequence data.[34]

Static CD Measurements. CD spectra were recorded with a J-600 circular dichroism polarimeter (JASCO, Tokyo, Japan). The sample conditions were 50 mM Gly-HCl (pH 2.0). Protein concentrations were 0.1 and 1 mg/mL for far- and near-UV measurements, respectively. The measurement temperature was 25 °C for checking the structure of the mutants (Figure 2) and 4 °C for the Gdn-HCl titration experiments (Figure 3). The instrumental parameters were as follows: data acquisition interval, 0.1 nm; scan rate, 20 nm/min; response, 4 s; bandwidth, 1 nm; number of accumulations, 4. For back-titration experiments (see Results), a protein solution containing 6.4 M Gdn-HCl was prepared. After overnight incubation at room temperature, the solution was diluted to various denaturant concentrations and the CD measurements were taken.

Kinetic CD Experiments. The refolding reaction was initiated by 8.5-fold dilution of a 7 mg/mL βLG solution containing 3.8 M Gdn-HCl and 50 mM Gly (pH 3.0) with dilution buffer [50 mM Gly (pH 3.0)]. The time course of ellipticity after the initiation of the refolding process was monitored at 14 wavelengths ranging from 210 to 250 nm. The measurements from 6.3 ms to 10 s were performed using a stopped-flow CD apparatus (model 400 CD spectrometer, AVIV Biomedical, Lakewood, NJ), whereas those from 10 s to 30 min were taken using a CD spectrometer (J-720, JASCO) with manual mixing. In addition, for E44L, the time-dependent spectral change after 30 min was measured. The measurements were performed at 10 °C because of the limit of the thermostat of the apparatus.

Calculation of Amphiphilic Helical Potential. The helical hydrophobic moment ($\langle\mu_H\rangle$), a quantitative measure of helical amphiphilicity, was calculated according to the method of Chen et al.[14] using the equation

$$\langle\mu_{H,i}\rangle = \left\{ \left[\sum_{n=i-5}^{i+5} H_n \sin(\delta n) \right]^2 + \left[\sum_{n=i-5}^{i+5} H_n \cos(\delta n) \right]^2 \right\}^{1/2} / 11 \quad (1)$$

where $\langle\mu_{H,i}\rangle$ is the helical hydrophobic moment for the ith residue, δ is the angular rotation between residues as viewed down a helical axis (100° for an α-helix and 120° for an extended helix), and H_n is the hydrophobic value assigned to residue n. Hydrophobic values were assigned to each amino acid using the method of Eisenberg.[35]

RESULTS

Design of Mutants with a Modified α-Helical Propensity. The shuffling of a free SH group of Cys121 with other S−S bonds that occurs in experiments on βLG folding leads to low reversibility of the pH- and heat-denatured forms.[36−41] Thus, folding experiments with βLG have been performed mainly at low pH, where the disulfide exchange reaction becomes very slow.[24,26,42−44] Previously, we confirmed that a Cys121-substituted mutant of βLG (i.e., C121A) showed an increase in reversibility[31] and that the mutant allowed us to study the folding of βLG under various conditions. Here, we use this mutant in folding experiments as a pseudo-wild type.

As mentioned, the α-helical propensity of the sequence is thought to be coupled with the stability of the non-native folding intermediate. Thus, we designed amino acid sequences whose

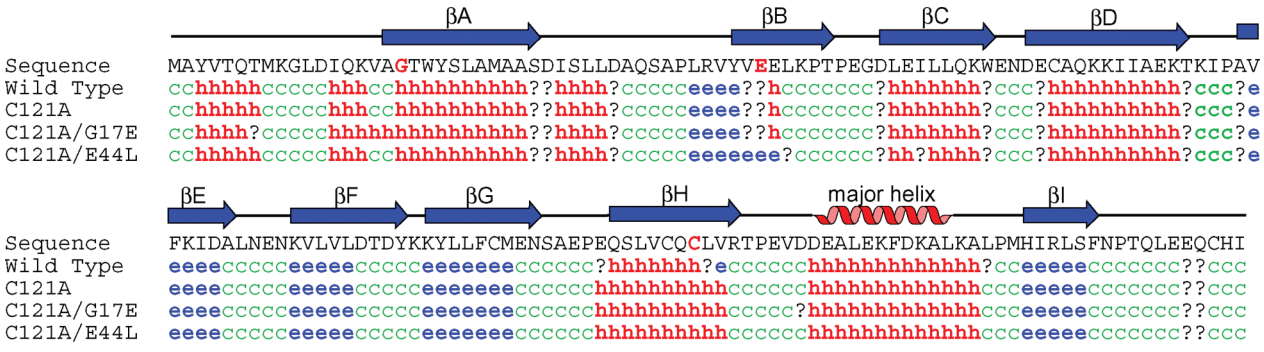

Figure 1. Predictions of secondary structure for each mutant. Predicted secondary structures are indicated by h (helix), e (sheet), t (turn), and c (coil). The probabilities were predicted with ANTHEPROT.[55] These results were the consensus of the results from GOR1, HNNC, MLRC, and Predator algorithms. Predictions made with each algorithm are shown in Figure 1 of the Supporting Information.

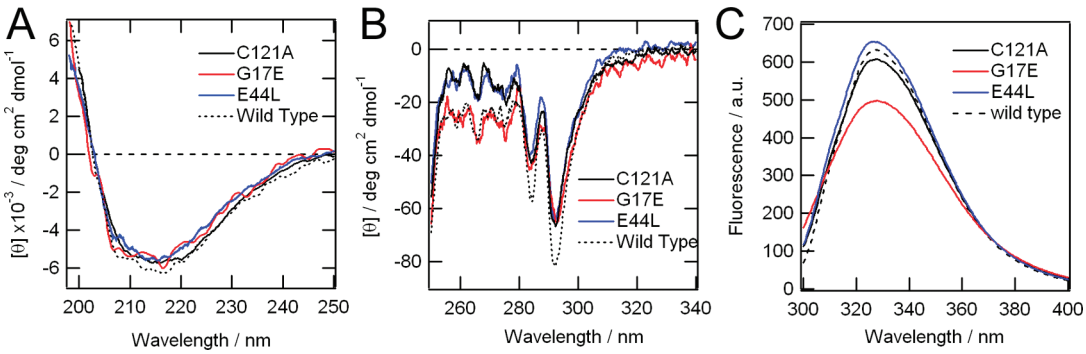

Figure 2. Structural comparisons of C121A, C121A/G17E, and C121A/E44L βLGs by (A) far-UV CD, (B) near-UV CD, and (C) fluorescence. In each panel, spectra of C121A, C121A/G17E, and C121A/E44L are colored black, red, and blue, respectively. As a reference, spectra of wild-type βLG are shown with dotted lines.

secondary structure propensity in the N-terminal region was modified. We chose two mutants, C121A/G17E (hereafter G17E) and C121A/E44L (hereafter E44L). Predictions of secondary structure are shown in Figure 1 and Figure 1 of the Supporting Information. It is predicted that G17E has a greater α-helical propensity at strand A with respect to the pseudo-wild type, whereas E44L has a higher β-propensity at strand B. From these predictions, it is assumed that the G17E and E44L mutations lead to stabilization and destabilization of the non-native intermediate, respectively.

We expressed the three mutants, C121A, G17E, and E44L, by using *E. coli*. We checked their structures by far- and near-UV CD and fluorescence spectroscopies. We found that their far- and near-UV CD spectra were almost indistinguishable from those of wild-type βLG (Figure 2A,B). In addition, the peak wavelengths of the fluorescence for all mutants were ∼330 nm (Figure 2C), which is a characteristic value for a buried tryptophan residue. It should be noted that a slight decrease in fluorescence intensity for G17E was observed probably because the introduction of a charged side chain, i.e., the carboxyl group of the glutamic acid, decreased the efficiency of the emission from Trp19, which is the main contributor to the fluorescence spectrum of βLG. These observations confirm that there are no significant structural modifications in the native structure.

Structural Stability of the Native and Intermediate Forms of the Mutants. Trifluoroethanol (TFE) is known to induce formation of the α-helical structure of proteins.[45] We checked the dependence on TFE of the secondary structure for the three mutants at pH 2.0 and 25 °C (Figure 2 of the Supporting Information). The results indicated cooperative transitions from the native to α-helical structure at ∼15% (v/v) TFE for all three mutants.

Then, Gdn-HCl-induced unfolding of the C121A, G17E, and E44L βLGs was monitored by CD in the absence and presence of TFE at 4 °C. It is reported that a non-native α-helical intermediate accumulates during chemical denaturation in the presence of TFE at a temperature lower than room temperature,[45] and that this equilibrium intermediate is identical to the kinetic intermediate.[29] Panels A−C of Figure 3 show the Gdn-HCl-dependent spectral changes of each mutant in the absence of TFE, and panels D−F of Figure 3 show those in the presence of 10% TFE. Figure 3 of the Supporting Information also shows the direct comparisons of spectra of each mutant at the same denaturant concentration, i.e., 0, 0.8, 3.2, 4.8, and 6.4 M Gdn-HCl. Panels G and H of Figure 3 show the Gdn-HCl dependence of the molecular ellipticity at 222 nm for each mutant in 0 and 10% TFE, respectively. Furthermore, to check the reversibility of the unfolding reactions, back-titration experiments, in which a protein solution containing 6.4 M Gdn-HCl was diluted to various denaturant concentrations, were performed for each mutant in the presence and absence of 10% TFE. The results are plotted in panels G and H of Figure 3 as crosses. The data agreed with original titration data, confirming the reversibility of the unfolding reactions for all mutants.

In the absence of TFE, C121A and E44L showed two-state unfolding (Figure 3G). On the other hand, G17E exhibited a

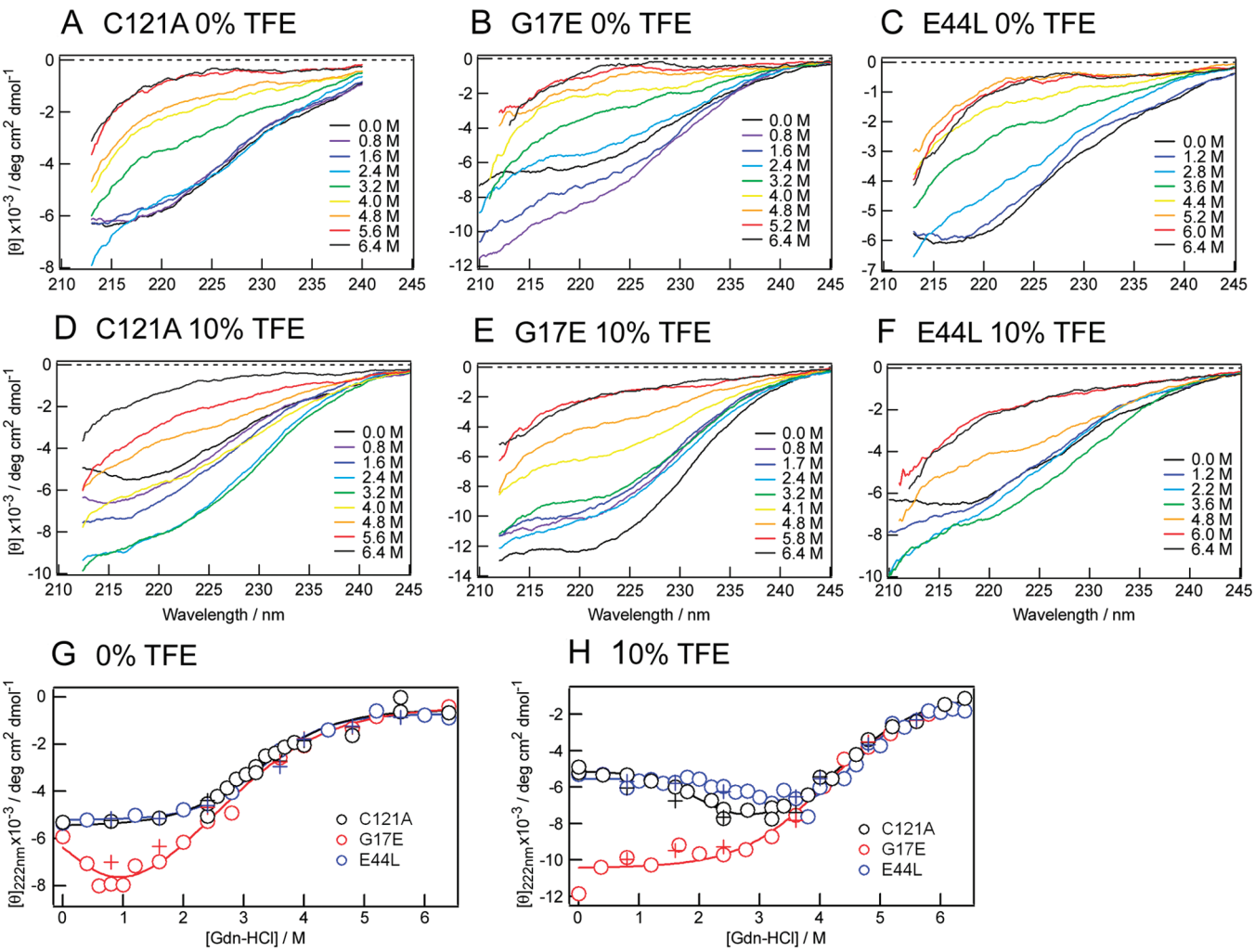

Figure 3. Gdn-HCl-dependent ellipticity of each mutant. The Gdn-HCl titration experiments were monitored by CD. (A−F) CD spectra of each mutant at various concentrations of Gdn-HCl in the absence of TFE (A−C) and in the presence of 10% TFE (D−F). (G and H) Gdn-HCl-dependent ellipticity at 222 nm in 0% (G) or 10% TFE (H) plotted for each mutant. The solid lines in G and H are the theoretical curves calculated from eq 7. The crosses are the results of back-titration experiments for confirming the reversibility of the unfolding.

minimum in ellipticity at ∼0.8 M Gdn-HCl, which indicates an accumulation of the intermediate (see Figure 3 of the Supporting Information). These results indicate that, in the case of G17E, the difference in energy between the intermediate and native forms is smaller than that for C121A. The intermediates of C121A and E44L might not be stable enough to significantly accumulate during the Gdn-HCl titration in the absence of TFE.

In the presence of 10% TFE, C121A and E44L exhibited minima in ellipticity at around 2.8 and 3.3 M Gdn-HCl, respectively, which indicates an increase in stability, and the subsequent accumulation of the intermediate (see Figure 3 of the Supporting Information). G17E showed an apparent two-state transition. However, the ellipticity at 0 M Gdn-HCl (ca. −10000) was markedly greater in magnitude than that of the native structure at 0% TFE (ca. −5500). Thus, at 10% TFE, the Gdn-HCl-induced unfolding of G17E starts from the intermediate.

The Gdn-HCl-dependent changes in the ellipticities at various wavelengths were simultaneously analyzed by curve fitting. For the unfolding transition of βLG mutants, we assumed either a two-state (N and U or I and U) or three-state (N, I, and U) mechanism. In the case of the three-state model, the equilibrium constants between N and U or I and U were represented by

$$K_{NU} = exp\left(-\frac{\Delta G_{NU,0} + m_{NU}[\text{Gdn-HCl}]}{RT}\right) \quad (2)$$

$$K_{IU} = exp\left(-\frac{\Delta G_{IU,0} + m_{IU}[\text{Gdn-HCl}]}{RT}\right) \quad (3)$$

where $\Delta G_{NU,0}$ and $\Delta G_{IU,0}$ are the free energy changes of unfolding in the absence of Gdn-HCl, m_{NU} and m_{IU} are parameters for the cooperativity of unfolding, and R and T are the gas constant and absolute temperature, respectively. From these equilibrium constants, the fractions in the N, I, and U states (f_N, f_I, and f_U, respectively) are calculated as follows

$$f_N = K_{NU}/X \quad (4)$$

$$f_I = K_{IU}/X \quad (5)$$

$$f_U = 1/X \quad (6)$$

dx.doi.org/10.1021/bi200241a |*Biochemistry* 2011, 50, 6498–6507

Table 1. Stability of Each Mutant

sample	model	$\Delta G_{NU,0}$ (kJ/mol)	m_{NU} (kJ mol^{-1} M^{-1})	$\Delta G_{IU,0}$ (kJ/mol)	m_{IU} (kJ mol^{-1} M^{-1})
C121A, 0% TFE	two-state	−13.9 ± 0.1	3.87 ± 0.29		
G17E, 0% TFE	three-state	−7.8 ± 0.4	7.63[a]	−6.3 ± 0.2	2.50 ± 0.08
E44L, 0% TFE	two-state	−16.3 ± 1.3	4.93 ± 0.37		
C121A, 10% TFE	three-state	−23.0 ± 0.5	7.63 ± 0.20	−15.8 ± 0.5	3.57 ± 0.10
G17E, 10% TFE	two-state			−18.2 ± 1.0	4.38 ± 0.24
E44L, 10% TFE	three-state	−37.0 ± 3.0	9.18 ± 0.62	−28.1 ± 3.2	6.22 ± 0.69

[a] This value is fixed (see the text).

where $X = 1 + K_{IU} + K_{NU}$. The observed spectrum can be constructed from the equation

$$[\theta]([\text{Gdn-HCl}],\lambda) = f_N \times [\theta]_N(\lambda) + f_I \times [\theta]_I(\lambda) + f_U \times [\theta]_U(\lambda) \quad (7)$$

where λ is a wavelength. $[\theta]_N(\lambda)$ and $[\theta]_U(\lambda)$ are the spectra obtained at 0 and 6.4 M Gdn-HCl, respectively. It should be noted that we used $[\theta]_{I0}(\lambda)$, which is the estimated spectrum of the burst-phase intermediate state (I_0) from the stopped-flow experiment (see below), as $[\theta]_I(\lambda)$ in eq 7, because the I state in this equilibrium experiment is assumed to be identical to the I_0 state in a kinetic process. It is also noted that the m_{NU} value did not converge in the fitting of G17E in 0% TFE because there are not enough data points corresponding to the N state. Thus, the m_{NU} value was set to the same value as that for C121A in 10% TFE, because unfolding of C121A under these conditions showed a three-state transition and was assumed to have a similar conformational transition. The model applied for the analysis and fitting parameters obtained (Table 1) was validated by an independent Gdn-HCl titration experiment monitored by fluorescence (see the Supporting Information).

The results confirmed that the ΔG_0 value of the native form of G17E was decreased with respect to that of C121A, which leads to the accumulation of the intermediate of G17E during the Gdn-HCl titration even in the absence of TFE. It is interesting that the E44L mutation seems to stabilize both the native and intermediate conformations with respect to the wild type. This indicates that the increase in β-sheet propensity caused the stabilization of both forms.

CD Stopped-Flow Experiments. We observed the refolding of the mutants by using CD. The Gdn-HCl titration experiment revealed that C121A βLG assumes the native state at 0.45 M Gdn-HCl and unfolded state at 3.84 M Gdn-HCl in the absence of TFE (Figure 3G). Thus, refolding was initiated by 8.5-fold dilution of the unfolded protein in 3.84 M Gdn-HCl with 50 mM Gly-HCl (pH 2.0), which results in a final Gdn-HCl concentration of 0.45 M. All kinetic experiments were conducted at 10 °C because the folding kinetics would be too fast to monitor with the apparatus at room temperature.[24]

The refolding kinetics of the three mutants, as monitored by measuring the ellipticity at various wavelengths, are shown in Figure 4A−C. As previously reported for wild-type βLG, the CD intensity exceeded the native value within the dead time of the measurement (overshoot) and then returned slowly to the native value.[24,46] Similar overshoots observed here indicate that these mutants fold in a manner similar to that of the wild type.

To precisely characterize the folding process for each mutant, we determined the folding rate and ellipticity of each conformation from the experimental data. Refolding curves at various wavelengths (Figure 4A−C) were simultaneously analyzed by curve fitting with a theoretical equation that assumes one to three exponential phases after the burst phase.

$$[\theta](\lambda,t) = [\theta]_\infty(\lambda) + \sum_{i=1}^{n} A_i(\lambda)\, exp(-k_i t) \quad (8)$$

where $[\theta](\lambda,t)$ is the observed ellipticity at wavelength λ and time t, $[\theta]_\infty(\lambda)$ is the ellipticity at infinity, n is the number of observed phases, and $A_i(\lambda)$ and k_i are the amplitude and rate constant for the respective phases, respectively. It is noted that k_i is the global variable for all traces at any wavelength, whereas $A_i(\lambda)$ and $[\theta]_\infty(\lambda)$ were the specific variables for individual wavelengths. Then, the spectra for each state were calculated from A_i and $[\theta]_\infty$. For example, when $n = 2$, the spectrum of the I_0 state is calculated as $[\theta]_{I0}(\lambda) = [\theta]_\infty(\lambda) + A_1(\lambda) + A_2(\lambda)$. The apparent rate constants of the respective phases are listed in Table 2, and reconstructed spectra for the respective states are shown in Figure 4D−F. It is thought that the dimerization reaction is not involved in these phases because βLG exists as a monomer at acidic pH. It was confirmed that there is no dimerization process in the folding of wild-type βLG.[24]

We roughly estimated the secondary structure for the conformations identified in the kinetic experiment. We assumed the CD spectrum to be the sum of pure spectra of α-helix, β-sheet, and random coil structures, which leads to the following equation:

$$[\theta](\lambda) = f_\alpha \times [\theta]_\alpha(\lambda) + f_\beta \times [\theta]_\beta(\lambda) + f_R \times [\theta]_R(\lambda) \quad (9)$$

where $[\theta]_\alpha(\lambda)$, $[\theta]_\beta(\lambda)$, and $[\theta]_R(\lambda)$ are pure CD spectra of the α-helix, β-sheet, and random coil, respectively. f_α, f_β, and f_R are the fractions of each structure. We fitted the spectra of the identified forms to the equation to obtain f_α, f_β, and f_R. We quoted the spectra of the α-helix and β-sheet from Greenfield and Fasman[47] and assumed C121A at 6.4 M Gdn-HCl to have pure random-coil spectra. The fitting results are summarized in Figure 5 and Table 2 of the Supporting Information. This analysis revealed that the behaviors of the two mutants were significantly perturbed. It should be noted that the secondary structure contents evaluated from this procedure might contain some error because the ellipticity data at <210 nm are not available because of the high absorbance of Gdn-HCl. However, as the changes in secondary structure content seem beyond the error, we can discuss the effect of the mutations on the intermediate structure.

C121A was found to refold with a two-phase process. The analysis of secondary structure confirmed that the burst-phase intermediate (I_0) of C121A has greater α-helical content than the native form, and that a decrease in α-helical content and increase in β-sheet content occurred concomitantly in the

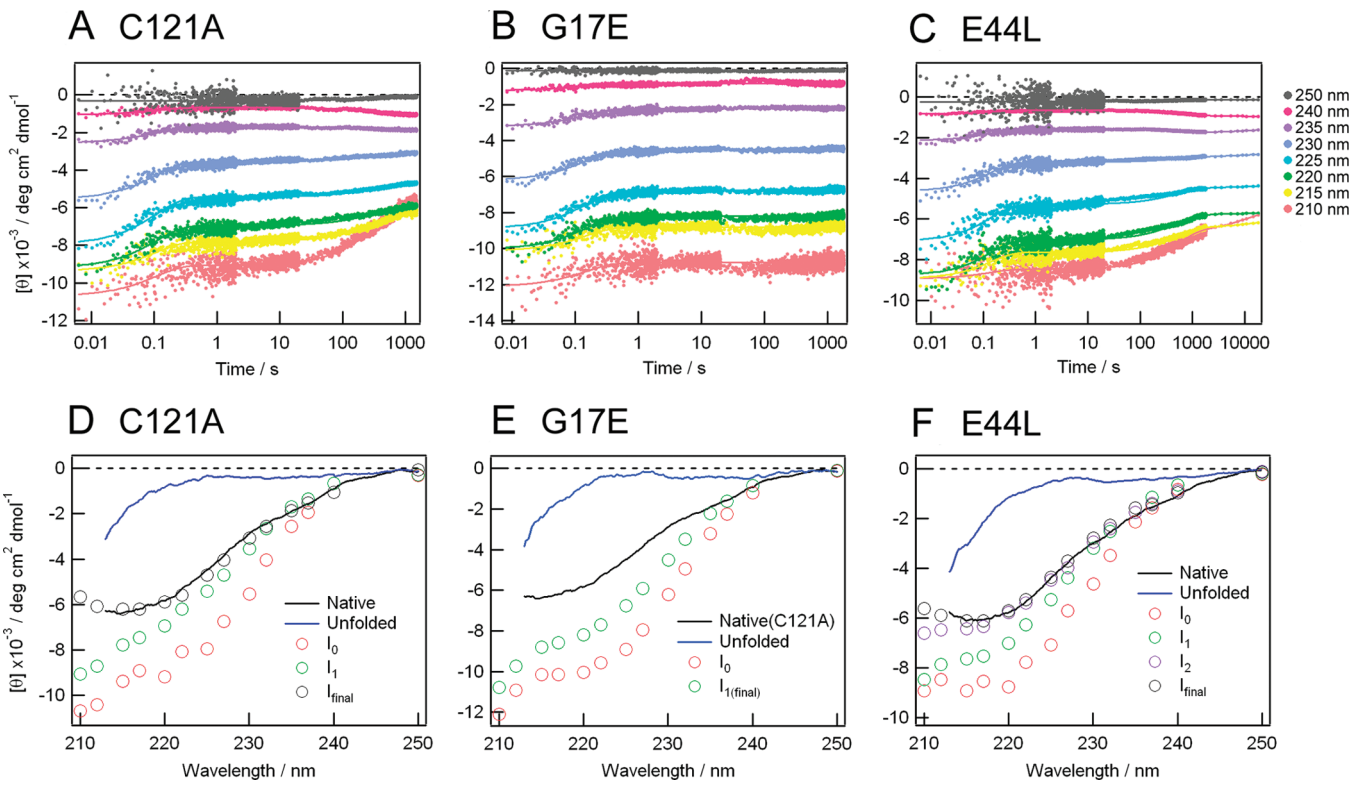

Figure 4. Refolding kinetics of C121A (A), G17E (B), and E44L (C) βLGs monitored by CD at various wavelengths. Data from the stopped-flow CD apparatus (6.3 ms to 10 s) and manual mixing experiment (10 s to 30 min) are linked. The raw data are represented by dots. The solid lines indicate the theoretical curves resulting from simultaneous fittings of the data at various wavelengths to eq 8, in which two- to four-state transitions are assumed in the folding processes. (D−F) Spectra corresponding to each kinetic state calculated from the results of the stopped-flow experiments for C121A (D), G17E (E), and E44L (F). In these panels, the circles indicate the calculated spectra and solid lines indicate the native (black) and denatured (blue) states.

Table 2. Kinetic Parameters Obtained from Stopped-Flow Experiments

	k_1 (s^{-1})	k_2 (s^{-1})	k_3 (s^{-1})
C121A	9.30 ± 0.11	$(2.76 \pm 0.02) \times 10^{-3}$	–
G17E	6.68 ± 0.08	–	–
E44L	7.15 ± 0.01	$(2.01 \pm 0.00) \times 10^{-3}$	$(9.03 \pm 0.00) \times 10^{-5}$

following phases ($I_0 \rightarrow I_1$ and $I_1 \rightarrow N$) (Figure 5 and Table 2 of the Supporting Information). This process is the same as that observed for wild-type βLG, which further confirmed that C121A can be treated as a pseudo-wild type.

G17E also exhibited a burst-phase intermediate with a non-native α-helical structure. Of note, the α-helical content of burst-phase intermediates of G17E was greater than that of C121A. This observation confirmed that the α-helical structure is more favorable for G17E than C121A, consistent with the prediction of secondary structure. G17E βLG exhibited single-phase refolding. After the burst-phase intermediate, decreases in α-helical content and a concomitant increase in β-sheet content were also observed. However, G17E did not reach a completely folded state. In this experiment, 0.45 M denaturant remained after the dilution. Under these conditions, the stability of the intermediate of G17E is comparable to that of the native form (Figure 3G).

E44L also exhibited behavior different from that of C121A. E44L showed a three-phase folding reaction. Although the rate constants for the first two steps were similar to those of C121A, that for the third phase was 20-fold slower. The folding intermediates of E44L had less α-helical content than those of C121A, consistent with the prediction of secondary structure. The burst-phase intermediate of E44L (I_0) contained 11.0% α-helix and 22.9% β-sheet. The β-sheet content is similar to that of I_1, I_2, and the native form but much greater than that of intermediates of C121A and G17E. These results indicate that the folding of E44L adopts a different route. The significant retardation of folding was probably associated with the increase in the β-sheet content of the burst-phase intermediate.

DISCUSSION

Figure 5 shows that C121A βLG first assumes I_0, which contains non-native α-components (Figure 5, black line). Then, the α-component decreases with a concomitant increase in the β-component from I_0 to N via I_1, as reported for wild-type βLG.[24] G17E βLG has the burst-phase intermediate with greater α-helical content, whereas it also shows a decrease in the α-component with a concomitant increase in the β-component. On the other hand, the burst-phase intermediate of E44L βLG had as much of the β-component as the native form did. Then, via several intermediates with fewer α-components, it achieved the native state. Thus, the pathways of both G17E and E44L seem slightly different from that of C121A.

A detailed folding process of βLG was proposed on the basis of the previous experimental results.[26] Adding some new pictures based on our results, we propose a modified scenario of βLG folding as follows (Figure 6, middle row). (i) The first step is the accumulation of the burst-phase intermediate (I_0), in which

dx.doi.org/10.1021/bi200241a |*Biochemistry* 2011, 50, 6498–6507

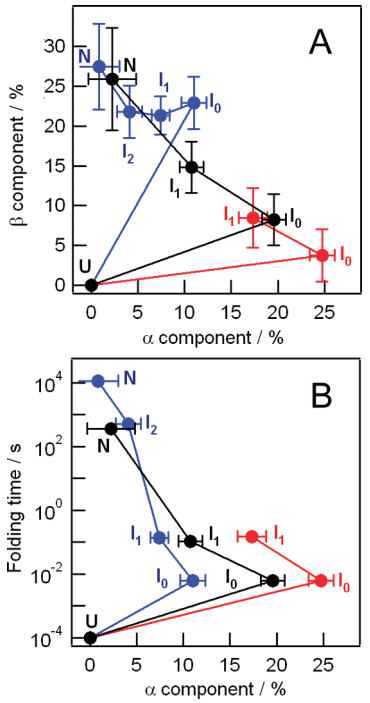

Figure 5. Plots of the estimated α- and β-contents of each kinetic state for each mutant. The folding time dependence of the secondary structure is shown. (A) α- and β-components for each kinetic state, which were obtained by decomposition analysis (see the text). (B) Transition times (i.e., $1/k$) plotted vs the α-component. The red, blue, and black lines correspond to the data for G17E, E44L, and C121A, respectively.

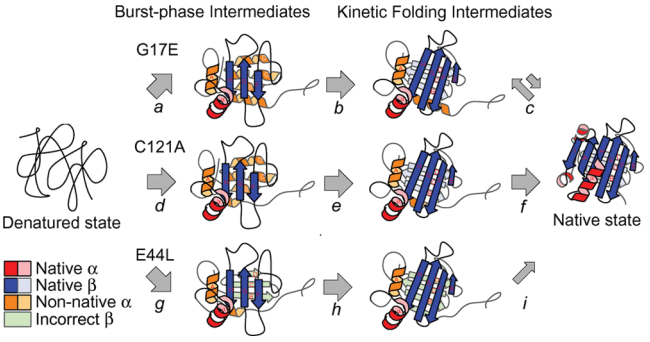

Figure 6. Schematic representation of the proposed process of βLG folding. A series of kinetic states are illustrated for G17E (top row), C121A (middle row), and E44L (bottom row). α- and β-structures seen in the native conformation are colored red and blue, respectively. Non-native α- and incorrect β-structures are colored orange and green, respectively.

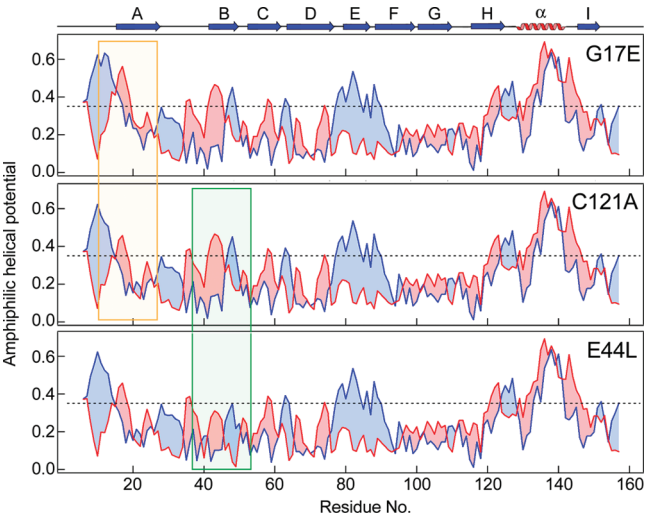

Figure 7. Amphiphilic helical potential at periods of 3.6 (red) and 3.0 (blue) residues/turn in each mutant. The $y = 0.35$ horizontal line reflects a "cutoff" value set roughly at a point where three or more consecutive values that exceed that potential are indicative of native amphiphilic α-helices in α-helical proteins.[14] Areas in which the amphiphilic α-helical potential exceeds the amphiphilic extended helical potential are shaded light red. Areas in which the amphiphilic extended helical potential exceeds the amphiphilic extended α-helical potential are shaded light blue. The orange and green boxes indicate the positions of the mutations of G17E and E44L, respectively.

non-native α-helices at strands A−D and core β-sheets at strands F−H are concomitantly formed. (ii) Propagation of β-sheet formation occurs from the core F−H sheet as the template. The formation of strands B−E might proceed through either the sequential development of hydrogen bonds or interactions of hydrophobic side chains oriented toward the inside of the central cavity. (iii) Finally, conversion of the non-native helix A to a β-strand is induced by the remainder of the molecule. This conclusion was reached on the basis of the discussions described below.

Effect of the G17E Mutation. The G17E mutation was predicted to increase the propensity for the α-structure at strand A. The quenched-flow experiment followed by nuclear magnetic resonance (NMR) measurements performed by Kuwata et al.[26] revealed a non-native α-helix in strand A region. The α-components of the burst-phase intermediates of C121A and G17E made up 19.6 and 24.8% of the total, respectively. Thus, the difference was attributed to the increased stability of helix A.

In the folding of C121A and G17E, a similar process follows the burst phase. However, G17E βLG was trapped as I_1 in the folding pathway and could not adopt the native conformation (steps *c* and *f* in Figure 6). The incomplete conversion of I_1 to N observed in the folding of G17E might come from overstabilization of helix A. The final step in the folding of βLG might correspond to the breaking of the α-helix and concomitant conversion to β-strands in the strand A region, which might be induced by the formation of the rest of the molecule, probably strand B, through hydrogen bonds. It is thought that the overstabilization of the non-native α-helix at strand A inhibits the conversion. Although it is necessary for an α-helix to form in this region, it is also a requisite that the α-helix be unstable as it must be converted in the later stages of the folding process.

There was no significant difference between the k_1 values for C121A βLG and G17E βLG (steps *b* and *e* in Figure 6), which suggests that no structural change involving the strand A region occurs in the step leading from I_0 to I_1. The decrease in α-content and the concomitant increase in β-content might be attributed to another region, probably the region of strands B−E. Kuwata et al.[26] reported a high α-helical propensity and the absence of strong protection in this region. From these reports, the region of strands B−E might assume non-native, fluctuating helices, which can be observed with CD.

Effect of the E44L Mutation. E44L exhibited three-state folding. It is characteristic that the β-content of I_0 was as great

dx.doi.org/10.1021/bi200241a |*Biochemistry* 2011, 50, 6498–6507

as that of the native structure with slightly more α-content. From I_0 to the native conformation, a decrease in α-helical content was observed.

Although the β-content of I_0 was as great as that of the native form, E44L took longer to fold than C121A. Thus, the β-structure formed in the burst-phase intermediate is thought to have incorrect hydrogen bonds or wrong side chain packing (step *g* in Figure 6). It is possible that they include intermolecular interactions as well as intramolecular ones. Such incorrect structures might occur when the region of strands A−D solely forms β-sheet structure without any guide or template. This state seems a glasslike state, in which non-native interactions can still be somewhat stabilizing.[48] Previously, we reported that the disulfide-linked βLG dimers assume such a glassy state in its folding process. The trapped state appears after the formation of the core region in the burst phase and assumes considerable secondary and tertiary structures with additional non-native interactions between the monomers.[7] In the case of E44L, various structures with the wrong registration of hydrogen bonding, each of which corresponds to a local minimum, are formed at the I_0 state and remain present until the I_2−N conversion step occurs. As these structures lead to a rugged surface of the energy landscape, it takes time to escape from these states with incorrect β-sheet structures. On the other hand, in the native conformation, the high β-propensity gives additional stability as β-strands with hydrogen bonds are stabilized. Therefore, although the high β-propensity gives a highly stable native structure, it inhibits rapid folding because it can lead to incorrect interactions. The high α-helical propensity of the N-terminal half of the βLG sequence might shift the folding pathways around such a kinetic trap.

It should be noted that the points discussed above are further supported by Lim's theory in terms of the importance of the non-native intermediate for the α−β transition and the changes in the stabilities and structures of the intermediate states caused by the mutations.[14,16] This theory suggests that the region with high potential for the extended helix is the starting point of the transformation from the helical to sheet structure, whereas high potential for the α-helix prevents the transformation to slow the folding. Figure 7 shows amphiphilic helical potentials for the α-helical and extended helical structures calculated from the βLG sequence with the methods of Chen et al.[14] The spanning region from strand F to H has no propensity to form the α-helix or extended helix, whereas the region from strand A to D has the potential to form both α-helices and extended helices, consistent with the finding that the strands F−H form a β-sheet core rapidly, whereas strands A−D form a helical structure followed by an α−β transition. It is interesting that strand E has high potential for the extended helix, suggesting that it forms after the β-sheet core, and then the α−β transition at strands A−D follows.

The amphiphilic helical potentials for G17E and E44L are shown in Figure 7 (top and bottom panels, respectively). The G17E mutation increases the potential for the α-helix rather than the extended helix (indicated by an orange box), supporting the enhanced stability of helix A and the prevention of the subsequent transition to the native state. On the other hand, the E44L mutation induces a loss of potential for amphiphilic helices (indicated by a green box), suggesting that the decrease in the level of transient formation of the helical structure enhances the rapid formation of the β-sheet structure.

Role of the α-Helical Intermediate of Wild-Type βLG and Other β-Sheet Proteins. It should be noted that the concepts of "on-pathway" and "obligatory" intermediates should be distinguished. Both are based on the energy landscape theory, in which there are uncountable fluxes from the unfolded ensemble to the native conformation. In the case of relatively simple proteins, we can assume a simplified sequential folding scheme (e.g., U → I → N) and the terms on- and off-pathway intermediate seem appropriate.[49,50] However, for more complex proteins, there will be more states on the energy surface, and each of them is interchangeable with other states. In such situations, it is difficult to define clearly whether individual states are on- or off-pathway intermediates. Because the folding of βLG is such a case, we focus only on whether the non-native intermediate of βLG is obligatory.

Our answer to the question mentioned above is that the non-native α-helical intermediate is not an obligatory intermediate. According to various reports,[51−53] some proteins potentially have multiple folding pathways and which pathway is followed varies depending upon the folding conditions and the presence of mutations. In such cases, there are multiple choices, leading to no obligatory intermediates. On the basis of this view, the I_0 states of C121A and E44L are on different pathways, and therefore, the non-native α-helical structure seen in the wild type is not an obligatory intermediate state. However, these pathways appear to be closely related and comprise similar events; i.e., a collapse of the polypeptide chain occurs during the burst phase,[30] and a rearrangement of the secondary structure occurs during the following steps. Therefore, C121A and E44L have similar folding rate constants. Multiple pathways of βLG folding were indicated in a previous report.[26]

However, the non-native α-helix contributes to suppression of the formation of an incorrect β-structure in the region of strands A−D. In the case of E44L, the total folding time was longer than that of the wild type because an incorrect β-structure is assumed to form. As described above, we suggest that the β-barrel of βLGs is formed in a stepwise manner; that is, the first step is the formation of the β-sheet consisting of strands E−H, and the second step is the formation of the other β-sheet consisting of strands A−D. At the first step, the non-native α-helices in strands A−D form as a result of the local secondary structure preference. Probably, the formation of the non-native α-helices in these regions has an important role in sequestering redundant donors and acceptors of the hydrogen bonds in these strands from strands E−H not to interrupt the formation of the core β-sheet. Kuwata et al.[26] also published a similar discussion about the significance of the α-helical intermediate. To confirm our suggestions and to obtain a more detailed picture of βLG folding, conformational changes at the residue level should be precisely investigated using NMR in the future.

Recently, Tsukamoto et al.[54] reported the folding of human tear lipocalin (HTL), one of the lipocalin proteins. Although the burst-phase intermediate of HTL also showed a large contraction in the radius of gyration, it does not contain significant α-helical content. Nevertheless, HTL accomplished its folding within 20 s, which is more rapid than that of wild-type βLG, whose folding time is more than 1000 s at 4 °C or 100 s at 20 °C.[26] From these results, they suggested that the non-native α-helical intermediate is unnecessary for the folding of lipocalins. However, according to Lim's theory, helical intermediates could not be observed because, although HTL has the potential to form the extended helix, it could just be refolding rapidly. This possibility needs to be tested with kinetic experiments in the presence of TFE like those that Chen et al.[14] have performed.

CONCLUSION

We addressed the significance of the non-native folding intermediate of βLG. We suggest that the formation of the non-native α-helices causes the folding pathways to circumvent accumulative misfolded species. In other words, the non-native intermediate channels the folding pathway away from nonproductive β-sheet formation. Moderate-sized proteins could adopt strategies by which such nonproductive intermediates are avoided. This strategy may be widely adopted by other proteins. It is likely that there are other strategies for the effective folding of proteins, and elucidating them will lead to a clearer understanding of protein folding mechanisms.

ASSOCIATED CONTENT

Supporting Information. Protocols, obtained spectra, and results of the analysis of additional Gdn-HCl titration experiments monitored by fluorescence (Methods, Figure 4, and Table 1, respectively), original data of the secondary predictions for each mutant (Figure 1), TFE dependencies of ellipticity of the mutants (Figure 2), rearranged presentation of the results of the Gdn-HCl titration experiment shown in Figure 3 (Figure 3), and summary of the secondary elements for the mutants in each state (Table 2). This material is available free of charge via the Internet at http://pubs.acs.org.

AUTHOR INFORMATION

Corresponding Author

*Institute for Protein Research, Osaka University, 3-2 Yamadaoka, Suita, Osaka 565-0871, Japan. Phone: +81-6-6879-8614. Fax: +81-6-6879-8616. E-mail: ygoto@protein.osaka-u.ac.jp.

Present Addresses

§Suntory Foundation for Life Sciences, Wakayamadai 1-1-1, Shimamoto-cho, Mishima-gun, Osaka 618-8503, Japan.

Author Contributions

K.S. and S.F. contributed equally to this work.

Funding Sources

This work was supported in part by Grants-in-Aid for Scientific Research and for Young Scientists (B) from the Japanese Ministry of Education, Science, Culture, and Sports.

ABBREVIATIONS

βLG, bovine β-lactoglobulin; Gdn-HCl, guanidine hydrochloride; CD, circular dichroism; TFE, 2,2,2-trifluoroethanol; HTL, human tear lipocalin.

REFERENCES

(1) Brockwell, D. J., and Radford, S. E. (2007) Intermediates: Ubiquitous species on folding energy landscapes? *Curr. Opin. Struct. Biol. 17*, 30–37.

(2) Dobson, C. M. (2004) Experimental investigation of protein folding and misfolding. *Methods 34*, 4–14.

(3) Capaldi, A. P., Kleanthous, C., and Radford, S. E. (2002) Im7 folding mechanism: Misfolding on a path to the native state. *Nat. Struct. Biol. 9*, 209–216.

(4) Nabuurs, S. M., Westphal, A. H., and van Mierlo, C. P. (2008) Extensive formation of off-pathway species during folding of an α-β parallel protein is due to docking of (non)native structure elements in unfolded molecules. *J. Am. Chem. Soc. 130*, 16914–16920.

(5) Rea, A. M., Simpson, E. R., Meldrum, J. K., Williams, H. E., and Searle, M. S. (2008) Aromatic residues engineered into the β-turn nucleation site of ubiquitin lead to a complex folding landscape, non-native side-chain interactions, and kinetic traps. *Biochemistry 47*, 12910–12922.

(6) Sutto, L., Latzer, J., Hegler, J. A., Ferreiro, D. U., and Wolynes, P. G. (2007) Consequences of localized frustration for the folding mechanism of the IM7 protein. *Proc. Natl. Acad. Sci. U.S.A. 104*, 19825–19830.

(7) Yagi, M., Kameda, A., Sakurai, K., Nishimura, C., and Goto, Y. (2008) Disulfide-linked bovine β-lactoglobulin dimers fold slowly, navigating a glassy folding landscape. *Biochemistry 47*, 5996–6006.

(8) Uzawa, T., Kimura, T., Ishimori, K., Morishima, I., Matsui, T., Ikeda-Saito, M., Takahashi, S., Akiyama, S., and Fujisawa, T. (2006) Time-resolved small-angle X-ray scattering investigation of the folding dynamics of heme oxygenase: Implication of the scaling relationship for the submillisecond intermediates of protein folding. *J. Mol. Biol. 357*, 997–1008.

(9) Dill, K. A., Bromberg, S., Yue, K., Fiebig, K. M., Yee, D. P., Thomas, P. D., and Chan, H. S. (1995) Principles of protein folding: A perspective from simple exact models. *Protein Sci. 4*, 561–602.

(10) Mayor, U., Guydosh, N. R., Johnson, C. M., Grossmann, J. G., Sato, S., Jas, G. S., Freund, S. M., Alonso, D. O., Daggett, V., and Fersht, A. R. (2003) The complete folding pathway of a protein from nanoseconds to microseconds. *Nature 421*, 863–867.

(11) Dyson, H. J., and Wright, P. E. (2004) Unfolded proteins and protein folding studied by NMR. *Chem. Rev. 104*, 3607–3622.

(12) Religa, T. L., Markson, J. S., Mayor, U., Freund, S. M., and Fersht, A. R. (2005) Solution structure of a protein denatured state and folding intermediate. *Nature 437*, 1053–1056.

(13) McLeish, T. C. (2005) Protein folding in high-dimensional spaces: Hypergutters and the role of nonnative interactions. *Biophys. J. 88*, 172–183.

(14) Chen, E., Everett, M. L., Holzknecht, Z. E., Holzknecht, R. A., Lin, S. S., Bowles, D. E., and Parker, W. (2010) Short-lived α-helical intermediates in the folding of β-sheet proteins. *Biochemistry 49*, 5609–5619.

(15) Chikenji, G., and Kikuchi, M. (2000) What is the role of nonnative intermediates of β-lactoglobulin in protein folding? *Proc. Natl. Acad. Sci. U.S.A. 97*, 14273–14277.

(16) Lim, V. I. (1974) Structural principles of the globular organization of protein chains. A stereochemical theory of globular protein secondary structure. *J. Mol. Biol. 88*, 857–872.

(17) Godovac-Zimmermann, J. (1988) The structural motif of β-lactoglobulin and retinol-binding protein: A basic framework for binding and transport of small hydrophobic molecules? *Trends Biochem. Sci. 13*, 64–66.

(18) Sawyer, L., and Kontopidis, G. (2000) The core lipocalin, bovine β-lactoglobulin. *Biochim. Biophys. Acta 1482*, 136–148.

(19) Brownlow, S., Morais Cabral, J. H., Cooper, R., Flower, D. R., Yewdall, S. J., Polikarpov, I., North, A. C., and Sawyer, L. (1997) Bovine β-lactoglobulin at 1.8 Å resolution: Still an enigmatic lipocalin. *Structure 5*, 481–495.

(20) Kuwata, K., Hoshino, M., Forge, V., Era, S., Batt, C. A., and Goto, Y. (1999) Solution structure and dynamics of bovine β-lactoglobulin A. *Protein Sci. 8*, 2541–2545.

(21) Uhrínová, S., Smith, M. H., Jameson, G. B., Uhrín, D., Sawyer, L., and Barlow, P. N. (2000) Structural changes accompanying pH-induced dissociation of the β-lactoglobulin dimer. *Biochemistry 39*, 3565–3574.

(22) Konuma, T., Sakurai, K., and Goto, Y. (2007) Promiscuous binding of ligands by β-lactoglobulin involves hydrophobic interactions and plasticity. *J. Mol. Biol. 368*, 209–218.

(23) Sakurai, K., Oobatake, M., and Goto, Y. (2001) Salt-dependent monomer-dimer equilibrium of bovine β-lactoglobulin at pH 3. *Protein Sci. 10*, 2325–2335.

(24) Hamada, D., Segawa, S., and Goto, Y. (1996) Non-native α-helical intermediate in the refolding of β-lactoglobulin, a predominantly β-sheet protein. *Nat. Struct. Biol. 3*, 868–873.

(25) Kuwata, K., Hoshino, M., Era, S., Batt, C. A., and Goto, Y. (1998) α→β transition of β-lactoglobulin as evidenced by heteronuclear NMR. *J. Mol. Biol. 283*, 731–739.

(26) Kuwata, K., Shastry, R., Cheng, H., Hoshino, M., Batt, C. A., Goto, Y., and Roder, H. (2001) Structural and kinetic characterization of early folding events in β-lactoglobulin. *Nat. Struct. Biol. 8*, 151–155.

(27) Hamada, D., Kuroda, Y., Tanaka, T., and Goto, Y. (1995) High helical propensity of the peptide fragments derived from β-lactoglobulin, a predominantly β-sheet protein. *J. Mol. Biol. 254*, 737–746.

(28) Kuroda, Y., Hamada, D., Tanaka, T., and Goto, Y. (1996) High helicity of peptide fragments corresponding to β-strand regions of β-lactoglobulin observed by 2D-NMR spectroscopy. *Folding Des. 1*, 255–263.

(29) Hamada, D., and Goto, Y. (1997) The equilibrium intermediate of β-lactoglobulin with non-native α-helical structure. *J. Mol. Biol. 269*, 479–487.

(30) Arai, M., Ikura, T., Semisotnov, G. V., Kihara, H., Amemiya, Y., and Kuwajima, K. (1998) Kinetic refolding of β-lactoglobulin. Studies by synchrotron X-ray scattering, and circular dichroism, absorption and fluorescence spectroscopy. *J. Mol. Biol. 275*, 149–162.

(31) Yagi, M., Sakurai, K., Kalidas, C., Batt, C. A., and Goto, Y. (2003) Reversible unfolding of bovine β-lactoglobulin mutants without a free thiol group. *J. Biol. Chem. 278*, 47009–47015.

(32) Doering, D. S., and Matsudaira, P. (1996) Cysteine scanning mutagenesis at 40 of 76 positions in villin headpiece maps the F-actin binding site and structural features of the domain. *Biochemistry 35*, 12677–12685.

(33) Sakurai, K., and Goto, Y. (2002) Manipulating monomer-dimer equilibrium of bovine β-lactoglobulin by amino acid substitution. *J. Biol. Chem. 277*, 25735–25740.

(34) Gill, S. C., and von Hippel, P. H. (1989) Calculation of protein extinction coefficients from amino acid sequence data. *Anal. Biochem. 182*, 319–326.

(35) Eisenberg, D., Schwarz, E., Komaromy, M., and Wall, R. (1984) Analysis of membrane and surface protein sequences with the hydrophobic moment plot. *J. Mol. Biol. 179*, 125–142.

(36) Burova, T. V., Choiset, Y., Tran, V., and Haertlé, T. (1998) Role of free Cys121 in stabilization of bovine β-lactoglobulin B. *Protein Eng. 11*, 1065–1073.

(37) Cupo, J. F., and Pace, C. N. (1983) Conformational stability of mixed disulfide derivatives of β-lactoglobulin B. *Biochemistry 22*, 2654–2658.

(38) Griko, Yu. V., and Kutyshenko, V. P. (1994) Differences in the processes of β-lactoglobulin cold and heat denaturations. *Biophys. J. 67*, 356–363.

(39) Schokker, E. P., Singh, H., Pinder, D. N., Noriss, G. E., and Creamer, L. K. (1999) Characterization of intermediates formed during heat-induced aggregation of β-lactoglobulin AB at neutral pH. *Int. Dairy J. 9*, 791–800.

(40) Carrotta, R., Bauer, R., Waninge, R., and Rischel, C. (2001) Conformational characterization of oligomeric intermediates and aggregates in β-lactoglobulin heat aggregation. *Protein Sci. 10*, 1312–1318.

(41) Croguennec, T., Bouhallab, S., Mollé, D., O'Kennedy, B. T., and Mehra, R. (2003) Stable monomeric intermediate with exposed Cys-119 is formed during heat denaturation of β-lactoglobulin. *Biochem. Biophys. Res. Commun. 301*, 465–471.

(42) Forge, V., Hoshino, M., Kuwata, K., Arai, M., Kuwajima, K., Batt, C. A., and Goto, Y. (2000) Is folding of β-lactoglobulin non-hierarchic? Intermediate with native-like β-sheet and non-native α-helix. *J. Mol. Biol. 296*, 1039–1051.

(43) Ragona, L., Catalano, M., Zetta, L., Longhi, R., Fogolari, F., and Molinari, H. (2002) Peptide models of folding initiation sites of bovine β-lactoglobulin: Identification of nativelike hydrophobic interactions involving G and H strands. *Biochemistry 41*, 2786–2796.

(44) Ragona, L., Fogolari, F., Romagnoli, S., Zetta, L., Maubois, J. L., and Molinari, H. (1999) Unfolding and refolding of bovine β-lactoglobulin monitored by hydrogen exchange measurements. *J. Mol. Biol. 293*, 953–969.

(45) Shiraki, K., Nishikawa, K., and Goto, Y. (1995) Trifluoroethanol-induced stabilization of the α-helical structure of β-lactoglobulin: Implication for non-hierarchical protein folding. *J. Mol. Biol. 245*, 180–194.

(46) Kuwajima, K., Yamaya, H., Miwa, S., Sugai, S., and Nagamura, T. (1987) Rapid formation of secondary structure framework in protein folding studied by stopped-flow circular dichroism. *FEBS Lett. 221*, 115–118.

(47) Greenfield, N., and Fasman, G. D. (1969) Computed circular dichroism spectra for the evaluation of protein conformation. *Biochemistry 8*, 4108–4116.

(48) Oliveberg, M., and Wolynes, P. G. (2005) The experimental survey of protein-folding energy landscapes. *Q. Rev. Biophys. 38*, 245–288.

(49) Capaldi, A. P., Ferguson, S. J., and Radford, S. E. (1999) The Greek key protein apo-pseudoazurin folds through an obligate on-pathway intermediate. *J. Mol. Biol. 286*, 1621–1632.

(50) Crespo, M. D., Simpson, E. R., and Searle, M. S. (2006) Population of on-pathway intermediates in the folding of ubiquitin. *J. Mol. Biol. 360*, 1053–1066.

(51) Cavagnero, S., Nishimura, C., Schwarzinger, S., Dyson, H. J., and Wright, P. E. (2001) Conformational and dynamic characterization of the molten globule state of an apomyoglobin mutant with an altered folding pathway. *Biochemistry 40*, 14459–14467.

(52) Haq, S. R., Jurgens, M. C., Chi, C. N., Koh, C. S., Elfstrom, L., Selmer, M., Gianni, S., and Jemth, P. (2010) The plastic energy landscape of protein folding: A triangular folding mechanism with an equilibrium intermediate for a small protein domain. *J. Biol. Chem. 285*, 18051–18059.

(53) Otzen, D. E., and Oliveberg, M. (1999) Salt-induced detour through compact regions of the protein folding landscape. *Proc. Natl. Acad. Sci. U.S.A. 96*, 11746–11751.

(54) Tsukamoto, S., Yamashita, T., Yamada, Y., Fujiwara, K., Maki, K., Kuwajima, K., Matsumura, Y., Kihara, H., Tsuge, H., and Ikeguchi, M. (2009) Non-native α-helix formation is not necessary for folding of lipocalin: Comparison of burst-phase folding between tear lipocalin and β-lactoglobulin. *Proteins 76*, 226–236.

(55) Deléage, G., Combet, C., Blanchet, C., and Geourjon, C. (2001) ANTHEPROT: An integrated protein sequence analysis software with client/server capabilities. *Comput. Biol. Med. 31*, 259–267.